Modelling Phase-resolved Spectra and Energy-dependent Light Curves of the Vela Pulsar to Scrutinize its GeV Emission Mechanism

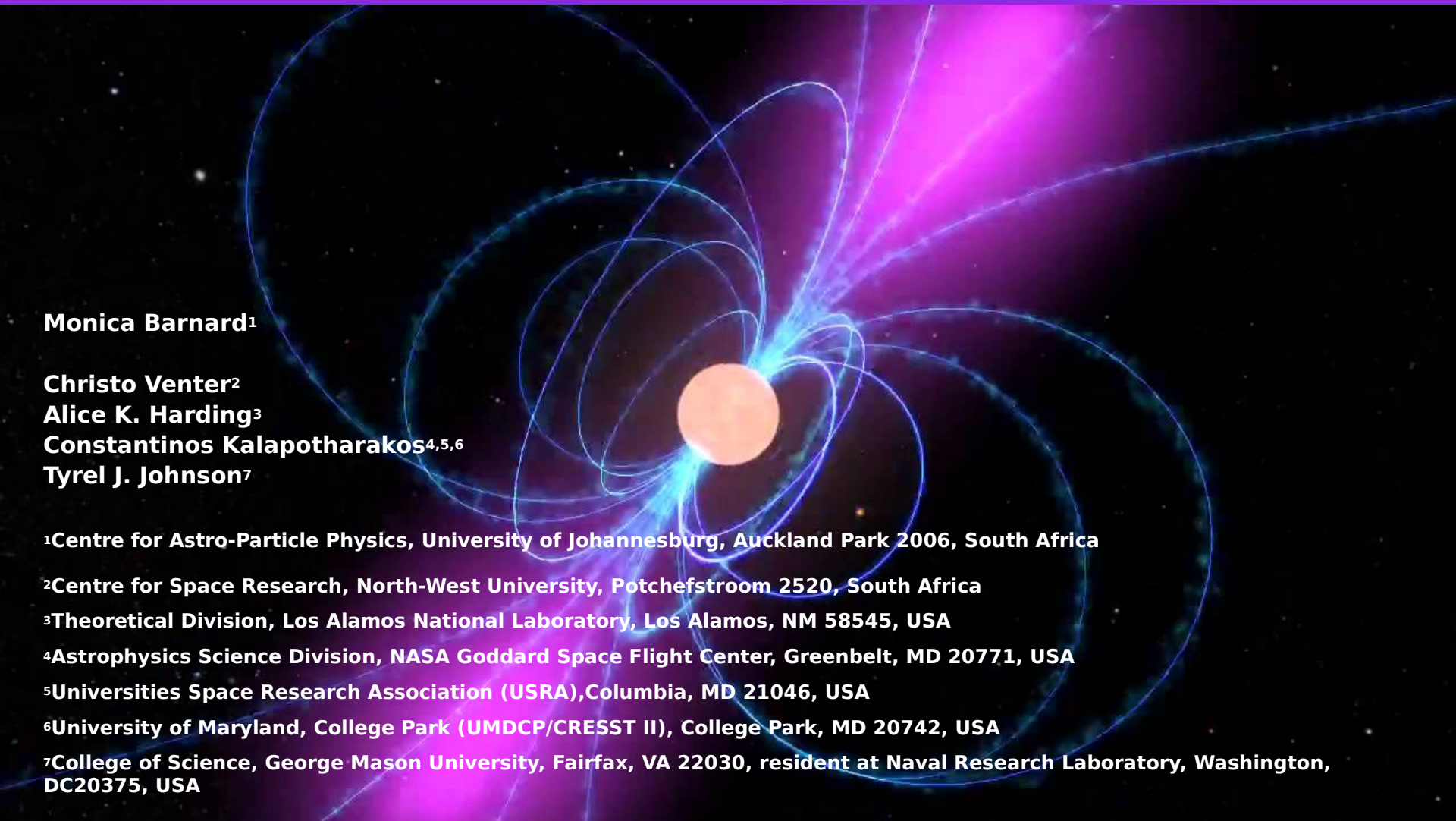

Monica Barnard[1]

Christo Venter[2]
Alice K. Harding[3]
Constantinos Kalapotharakos[4,5,6]
Tyrel J. Johnson[7]

[1]Centre for Astro-Particle Physics, University of Johannesburg, Auckland Park 2006, South Africa

[2]Centre for Space Research, North-West University, Potchefstroom 2520, South Africa

[3]Theoretical Division, Los Alamos National Laboratory, Los Alamos, NM 58545, USA

[4]Astrophysics Science Division, NASA Goddard Space Flight Center, Greenbelt, MD 20771, USA

[5]Universities Space Research Association (USRA),Columbia, MD 21046, USA

[6]University of Maryland, College Park (UMDCP/CRESST II), College Park, MD 20742, USA

[7]College of Science, George Mason University, Fairfax, VA 22030, resident at Naval Research Laboratory, Washington, DC20375, USA

Pulsars

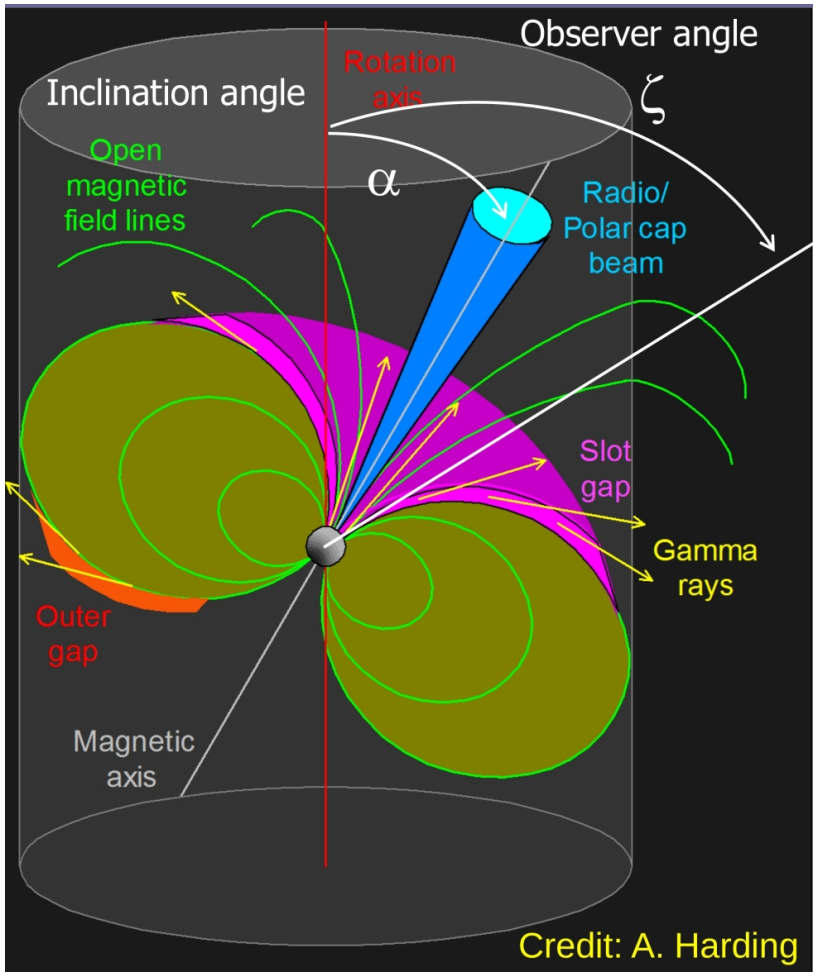

- A compact, highly magnetized neutron stars, rotating at tremendous rate (compared to a lighthouse).

- Typical values:
  - $R_{NS} \sim 12$ km.
  - $M_{NS} \sim 1.4M_{\odot}$ – $1.5M_{\odot}$ (up to $\sim 2.5M_{\odot}$ inferred for pulsars).
  - $B_0 \sim 10^8$ -10^{15} G (young pulsars – higher B).

- *Models:*
  - Traditional emission models:
    Polar Cap (Daugherty & Harding 1982),
    Slot Gap (Arons 1983),
    Outer Gap (Cheng et al. 1986),
    Pair-Starved Polar Cap (Harding et al. 2005).
  - Newer emission models:
    Striped-wind & Current-Sheet (Petri & Kirk 2003, Mochol & Petri 2015, Kalapotharakos et al. 2014),
    Annular gap (Du et al. 2012).

Observations of sub-TeV emission of Vela

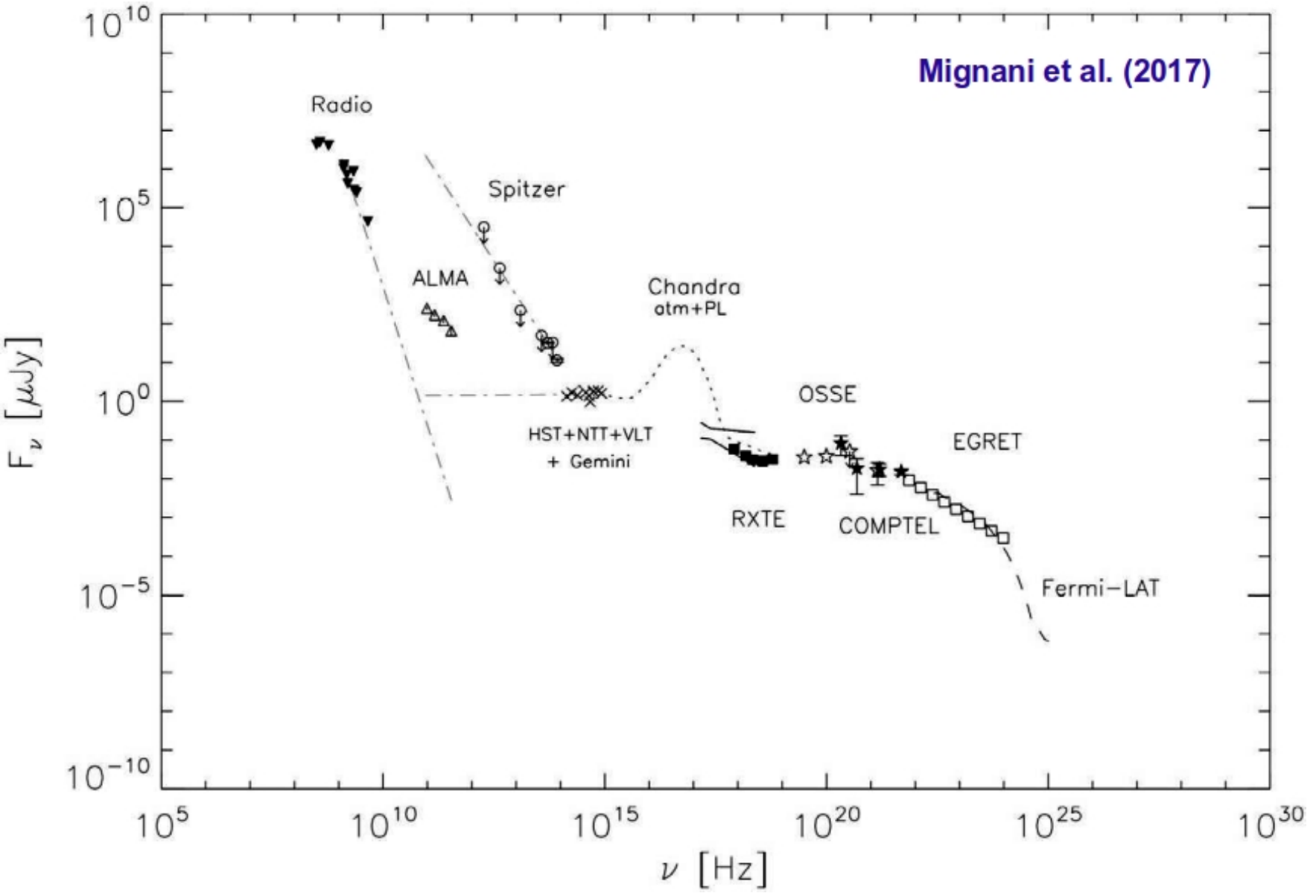

Observations of sub-TeV emission of Vela

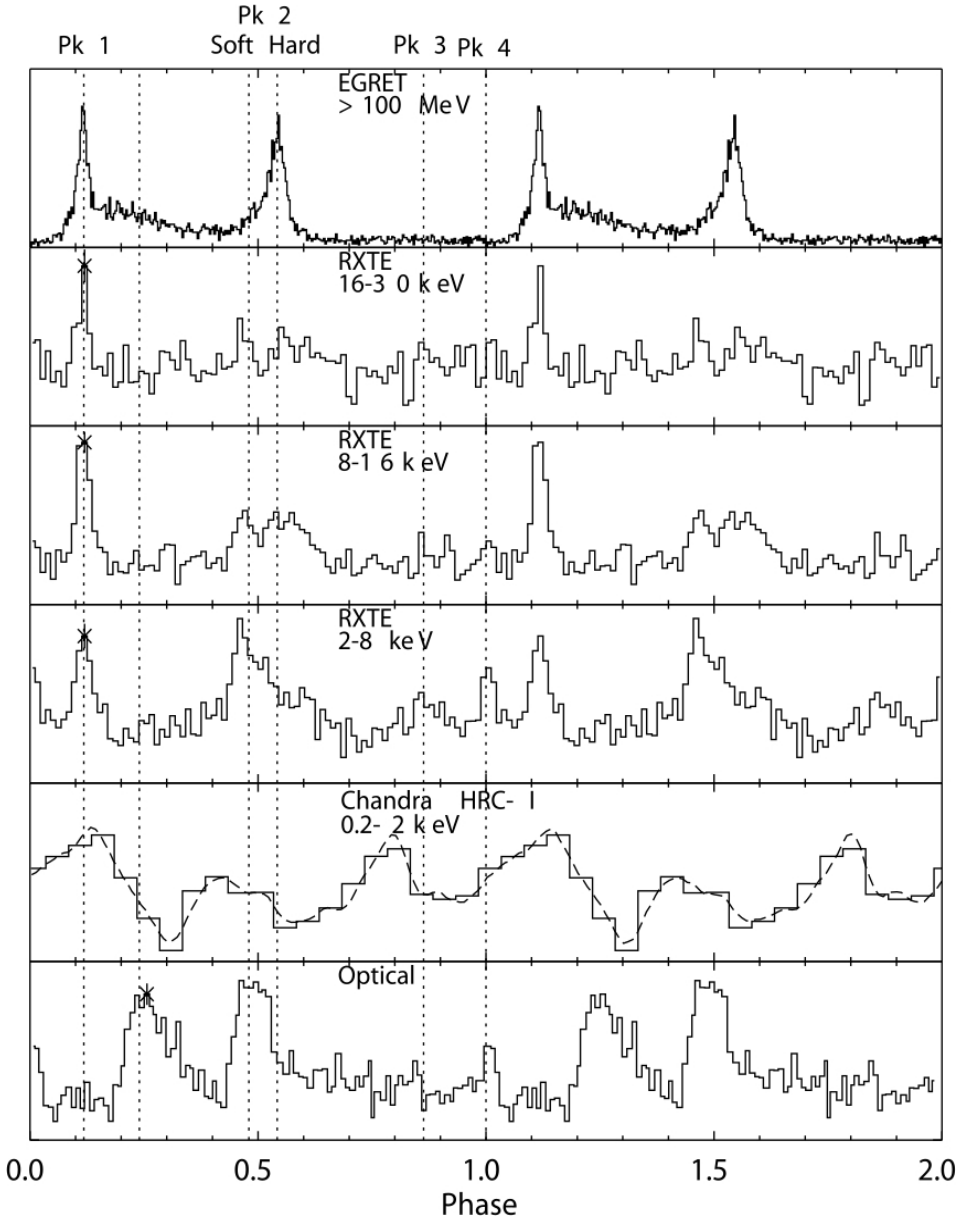

Harding et al. (2002)

Abdo et al. (2010)

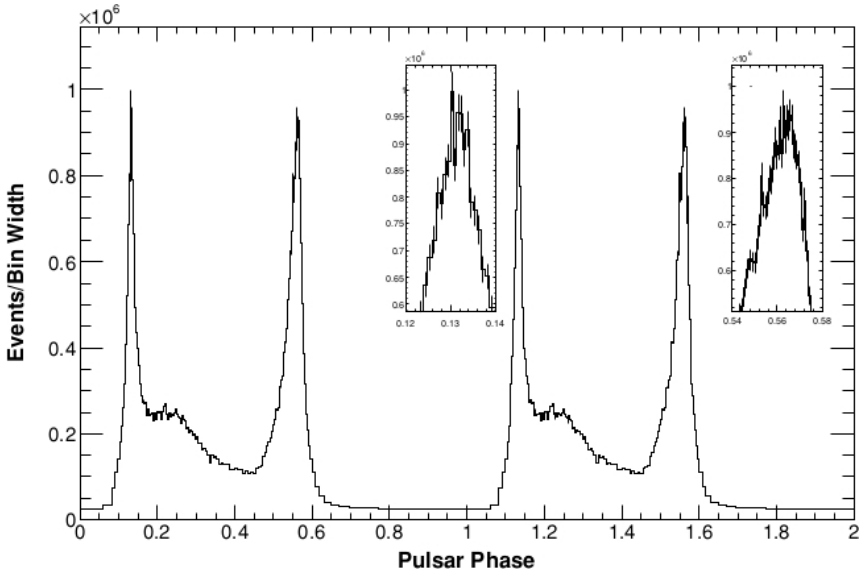

- Noticable trends vs. photon energy:
  - Flux ratio of the first peak (P1) relative to the second peak (P2) decreases.
  - Phase positions of peaks remain constant.
  - Pulses narrow with an increase in energy.
  - Evolution of bridge emission (decreases with energy and shifts in phase).

Observations of sub-TeV emission of Vela

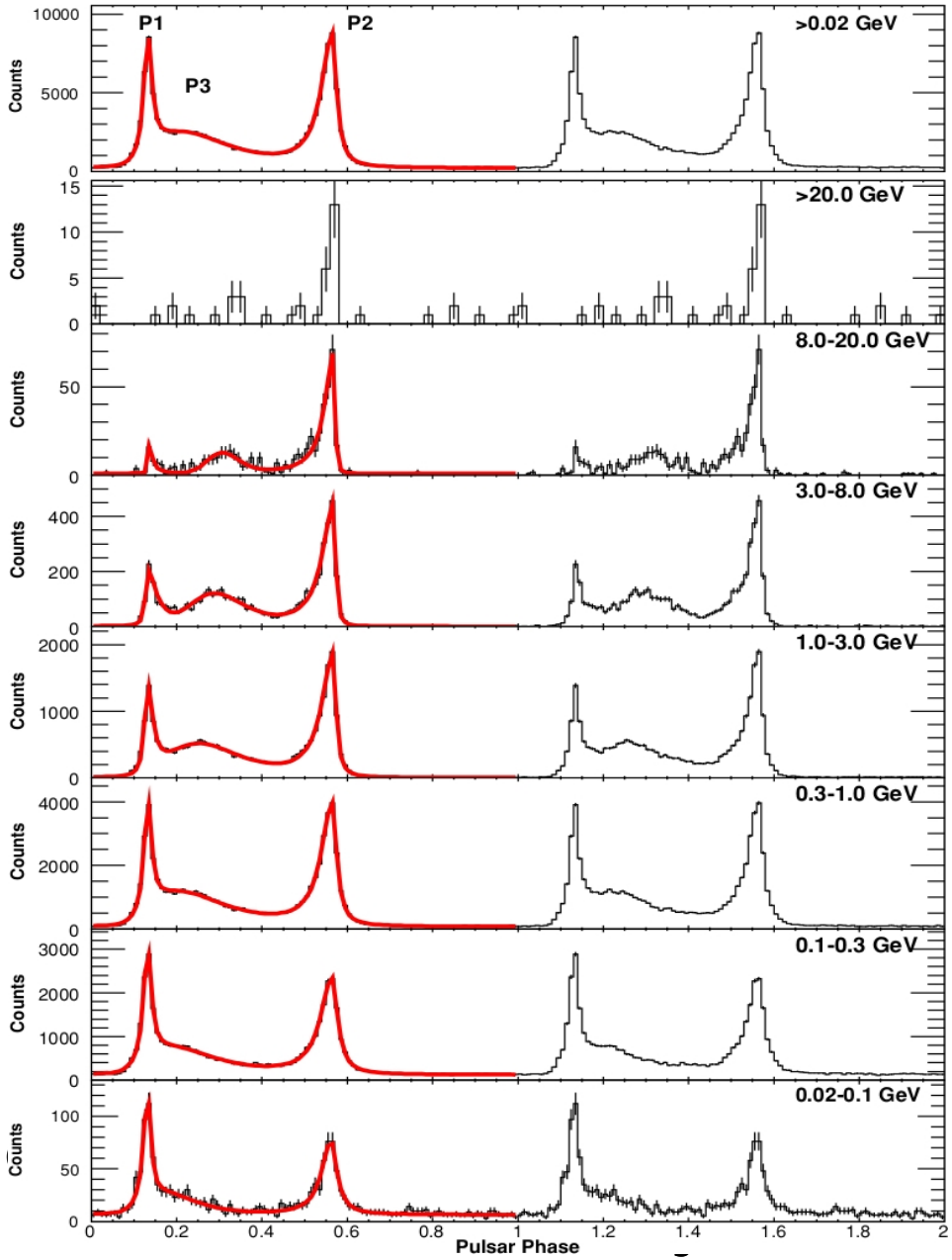

Abdo et al. (2010)

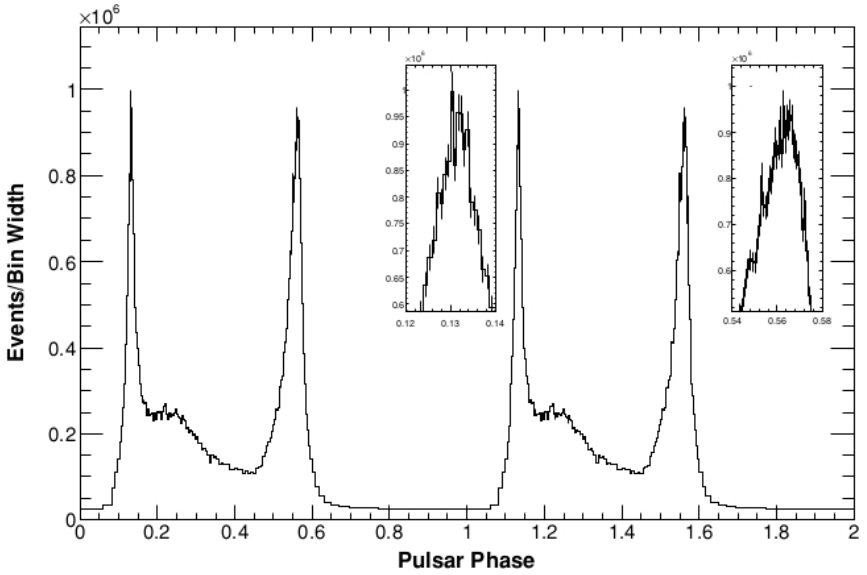

- Noticable trends vs. photon energy:
  - Flux ratio of the first peak (P1) relative to the second peak (P2) decreases.
  - Phase positions of peaks remain constant.
  - Pulses narrow with an increase in energy.
  - Evolution of bridge emission (decreases with energy and shifts in phase).

Observations of sub-TeV to TeV pulsar emission

- *Observations:*
  - *Fermi* LAT detected over 250 high-energy (> 100 MeV) gamma-ray pulsars.
  - Four pulsars detected by ground-based telescopes (IACTs) in the VHE range:

    Crab (Ansoldi et al. 2016): Up to 1 TeV

    Vela (Abdalla et al. 2018): Sub-20 GeV to 100 GeV (paper in prep. claiming up to 7 TeV). P2 detected at 5.6σ level and P1 not visible.

    Geminga (Acciari et al. 2020): Between 15 GeV and 75 GeV with 6.3σ for P2.

    PSR B1706-44 (Spir-Jacob et al. 2019): Sub-100 GeV.

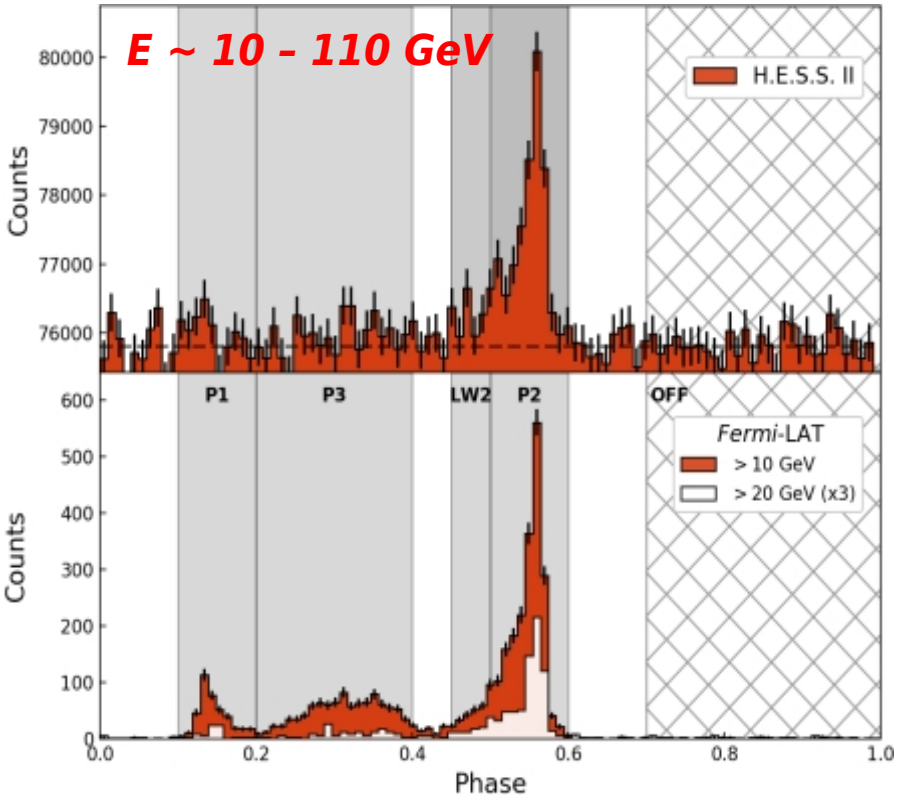

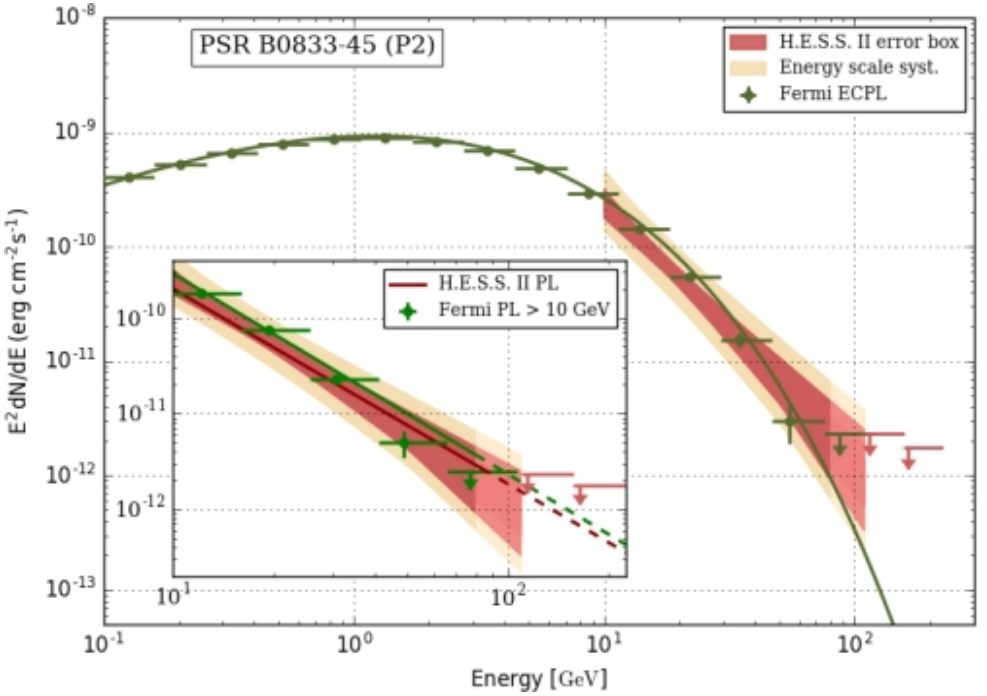

Abdalla et al. (2018)

Questions to be addressed

- Spectral shape of emitting particles?
- Which emission mechanisms contribute to the broadband SED?
- Local and global electrodynamical properties?
- Pulsar (magnetosphere) geometry?

Motivation

- Is the observed spectrum of H.E.S.S (>3σ for curvature emission) for Vela a continuation of the *Fermi* spectrum (curved sub-exponential) or a power law? Curvature radiation in GeV favoured at 3σ compared to a power-law shape. Additional VHE component distinct from GeV spectrum?
- H.E.S.S. and the *Fermi* LAT detection of Vela provide evidence for a curved GeV spectrum and recent kinetic simulations re-ignited the debate regarding the emission mechanism responsible for pulsed GeV-band emission (CR, SR or IC).
- We interpret this curved, GeV spectrum to be the result of curvature radiation due to primary particles in the pulsar magnetosphere accelerated predominantly in the current sheet.

SSC 3D emission model

Harding & Kalapotharakos (2015,2018)

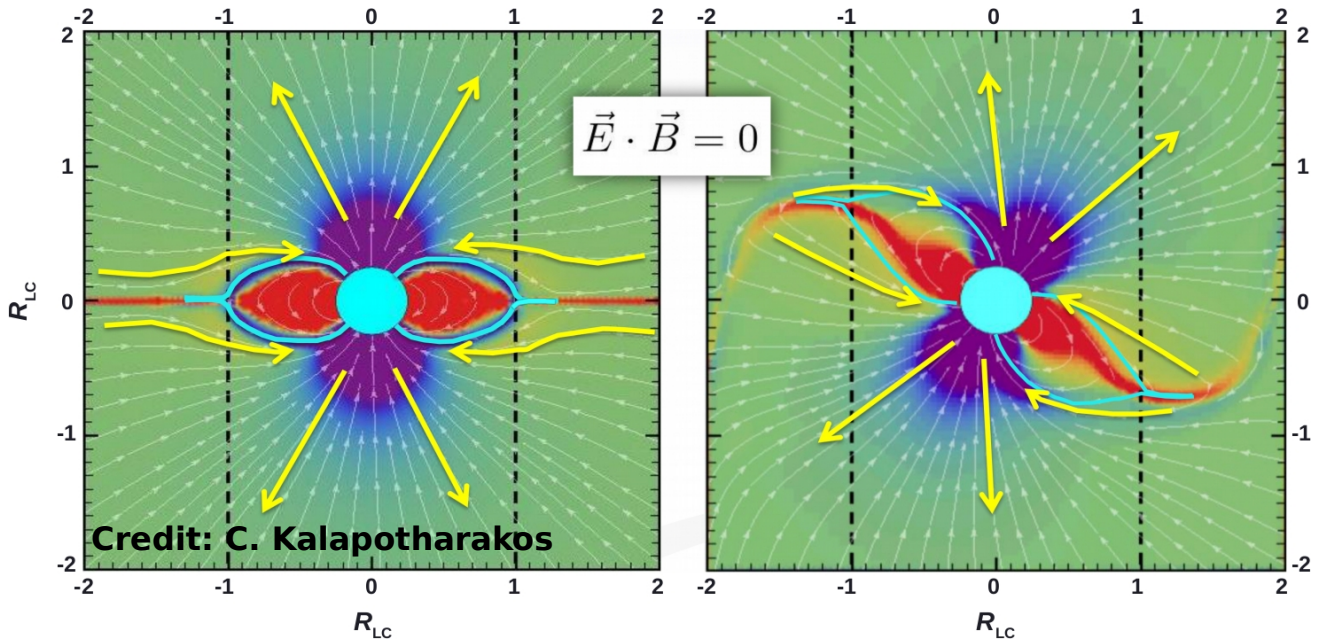

- Extended slot gap (SG) + 3D force-free magnetosphere (acceleration primarily in the current sheet and the *E*-field completely screened outside of the slot gap).

- Pairs from steady cascade in offset-PC *B*-field injected near stellar surface (Harding & Muslimov 2011a,b).

- Primaries accelerated in SG and current sheet (out to $r=2R_{LC}$) assuming a constant *E*-field - most emission comes from the current sheet (Mochol & Petri 2015). ***No pair acceleration.***

- One and two-step function for the accelerating *E*-field (latter motivated by kinetic simulations). $\boldsymbol{R_{acc} = eE_{||}/m_e c^2}$.

SSC 3D emission model

Harding & Kalapotharakos (2015,2018)

- Empirical radio core / cone model – resonant cyclotron absorption of radio photons (cf. Lyubarski & Petrova 1998) to regain pitch angles for synchrotron radiation (SR).
- Solve particle dynamics / transport.
- Radiation mechanisms:
  - Curvature.
  - Synchrotron.
  - Inverse Compton Scattering.
  - Synchrotron self-Compton.
  - Synchro-curvature (CR to SC in 2018 model).
- Inertial observer frame.
- Light curves and spectra.
- Transport:

$$\frac{d\gamma}{dt} = \frac{eE_{\parallel}}{mc} - \frac{2e^4}{3m^3c^5}B^2\,p_{\perp}^2 - \frac{2e^2\gamma^4}{3\rho_c^2} + \left(\frac{d\gamma}{dt}\right)^{\rm abs} - \left(\frac{d\gamma}{dt}\right)^{\rm SSC}$$

$$\frac{dp_{\perp}}{dt} = -\frac{3}{2}\frac{c}{r}p_{\perp} - \frac{2e^4}{3m^3c^5}B^2\,\frac{p_{\perp}^3}{\gamma} + \left(\frac{dp_{\perp}(\gamma)}{dt}\right)^{\rm abs}$$

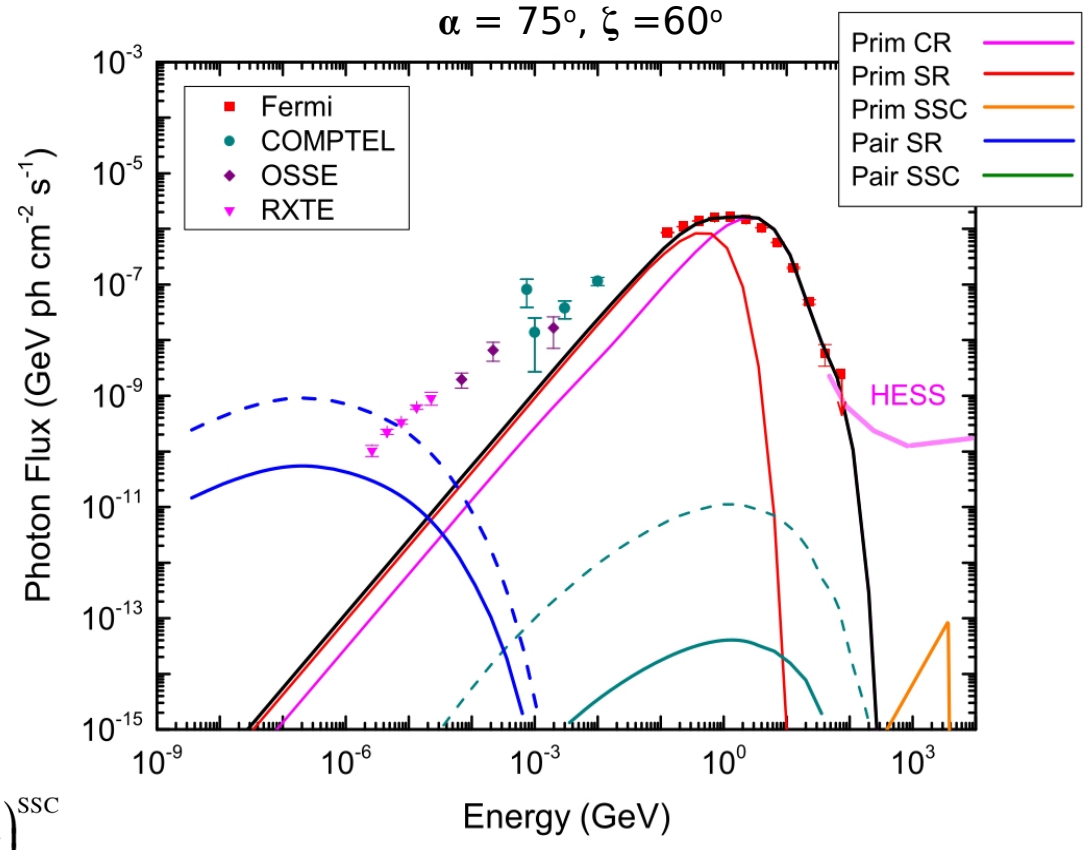

Harding et al. (2015)

SSC 3D emission model

Harding & Kalapotharakos (2015,2018)

- Empirical radio core / cone model – resonant cyclotron absorption of radio photons (cf. Lyubarski & Petrova 1998) to regain pitch angles for synchrotron radiation (SR).
- Solve particle dynamics / transport.
- Radiation mechanisms:
  - Curvature.
  - Synchrotron.
  - Inverse Compton Scattering.
  - Synchrotron self-Compton.
  - Synchro-curvature (CR to SC in 2018 model).
- Inertial observer frame.
- Light curves and spectra.
- Transport:

$$\frac{d\gamma}{dt} = \frac{eE_{\parallel}}{mc} - \frac{2e^4}{3m^3c^5}B^2\,p_{\perp}^2 - \frac{2e^2\gamma^4}{3\rho_c^2} + \left(\frac{d\gamma}{dt}\right)^{\rm abs} - \left(\frac{d\gamma}{dt}\right)^{\rm SSC}$$

$$\frac{dp_{\perp}}{dt} = -\frac{3}{2}\frac{c}{r}p_{\perp} - \frac{2e^4}{3m^3c^5}B^2\,\frac{p_{\perp}^3}{\gamma} + \left(\frac{dp_{\perp}(\gamma)}{dt}\right)^{\rm abs}$$

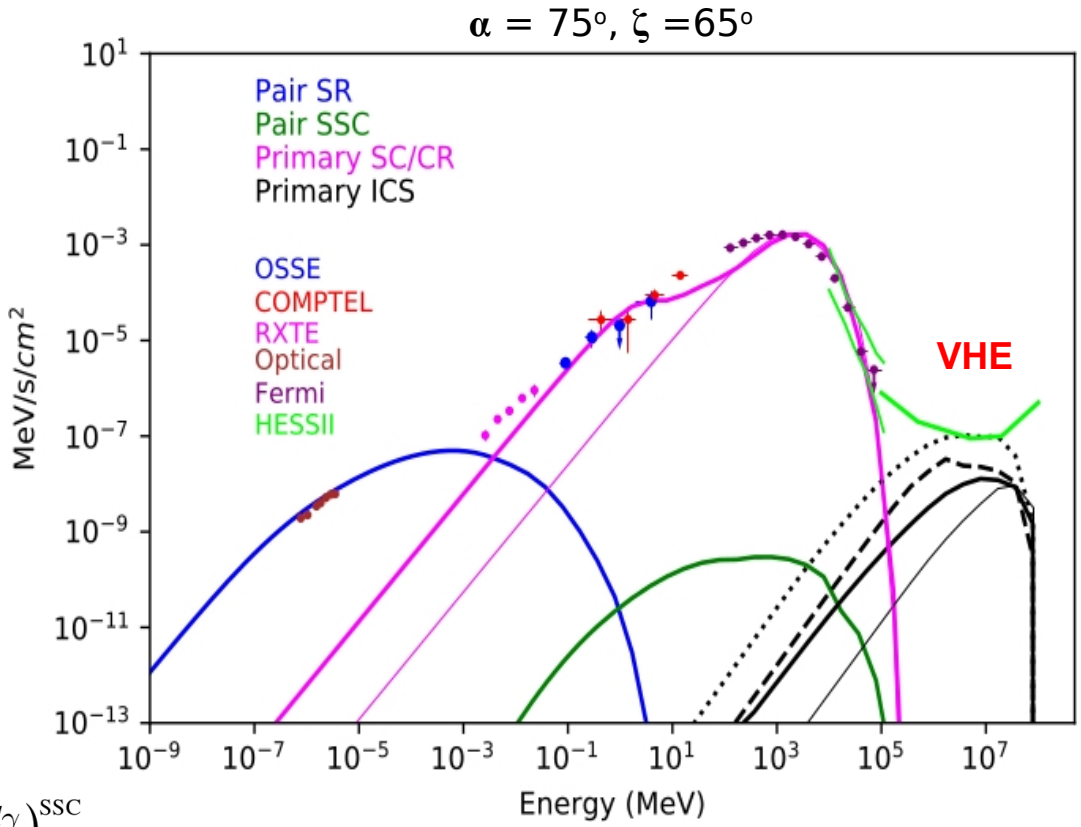

Harding et al. (2018)

Refinement of the curvature radius

Harding et al. (2015,2018), Barnard et al. (*submitted to ApJ*)

- One and two-step function for the accelerating *E*-field (latter motivated by kinetic simulations). $\boldsymbol{R_{acc} = eE_{||}/m_e c^2}$.
- Refined calculation of the curvature radius of particle trajectories - impacts the transport, light curves, and spectra.
- Did a small parameter study to find optimal parameters, i.e., α, ζ_{cut} , R_{acc} , and selected the best spatial resolution.

$\alpha = 75^o$

$\zeta_{cut} = 65^o$

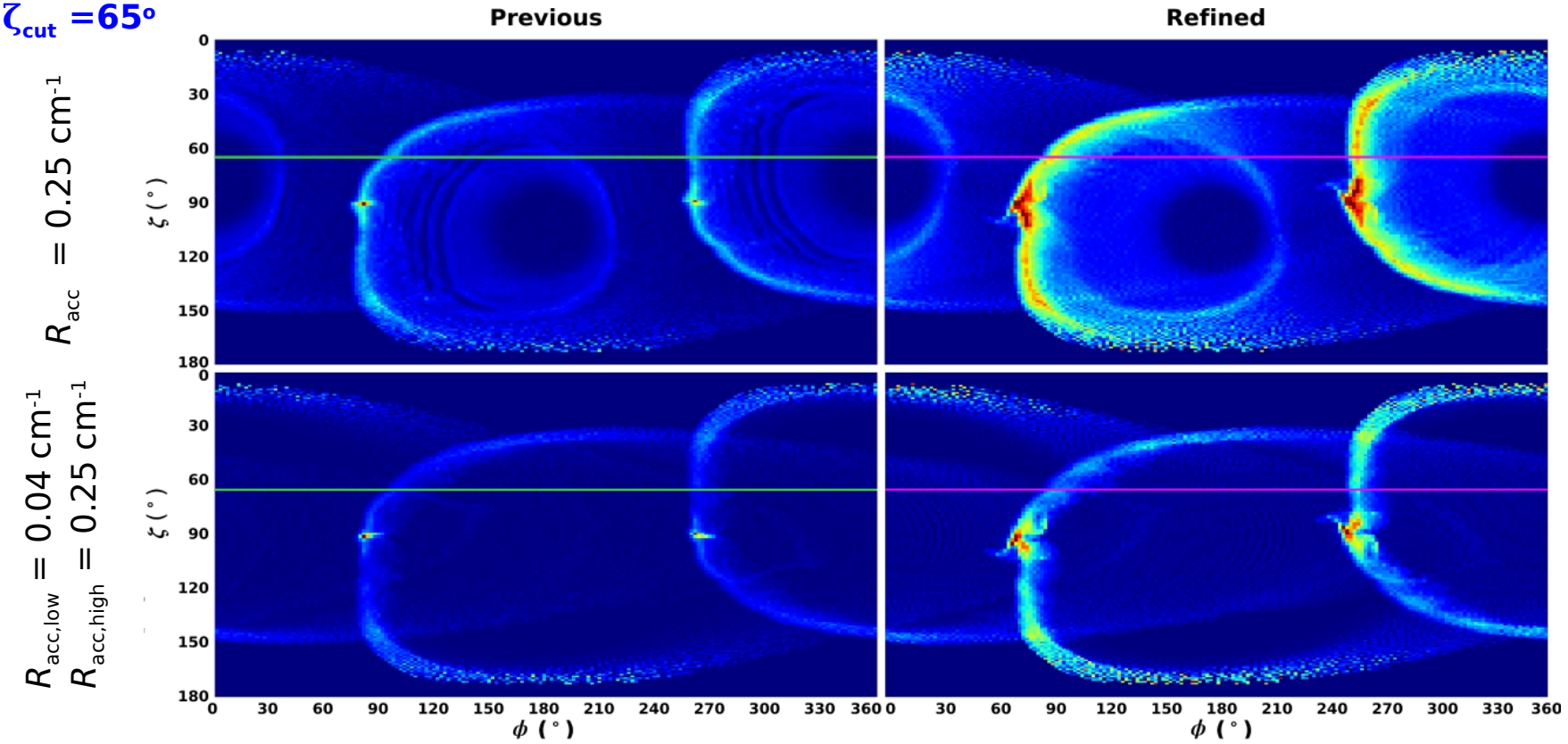

Energy-dependent curvature light curves

R_{acc} = 0.25 cm^{-1}

$R_{acc,low}$ = 0.04 cm^{-1}
$R_{acc,high}$ = 0.25 cm^{-1}

α = 75°
ζ_{cut} = 65°

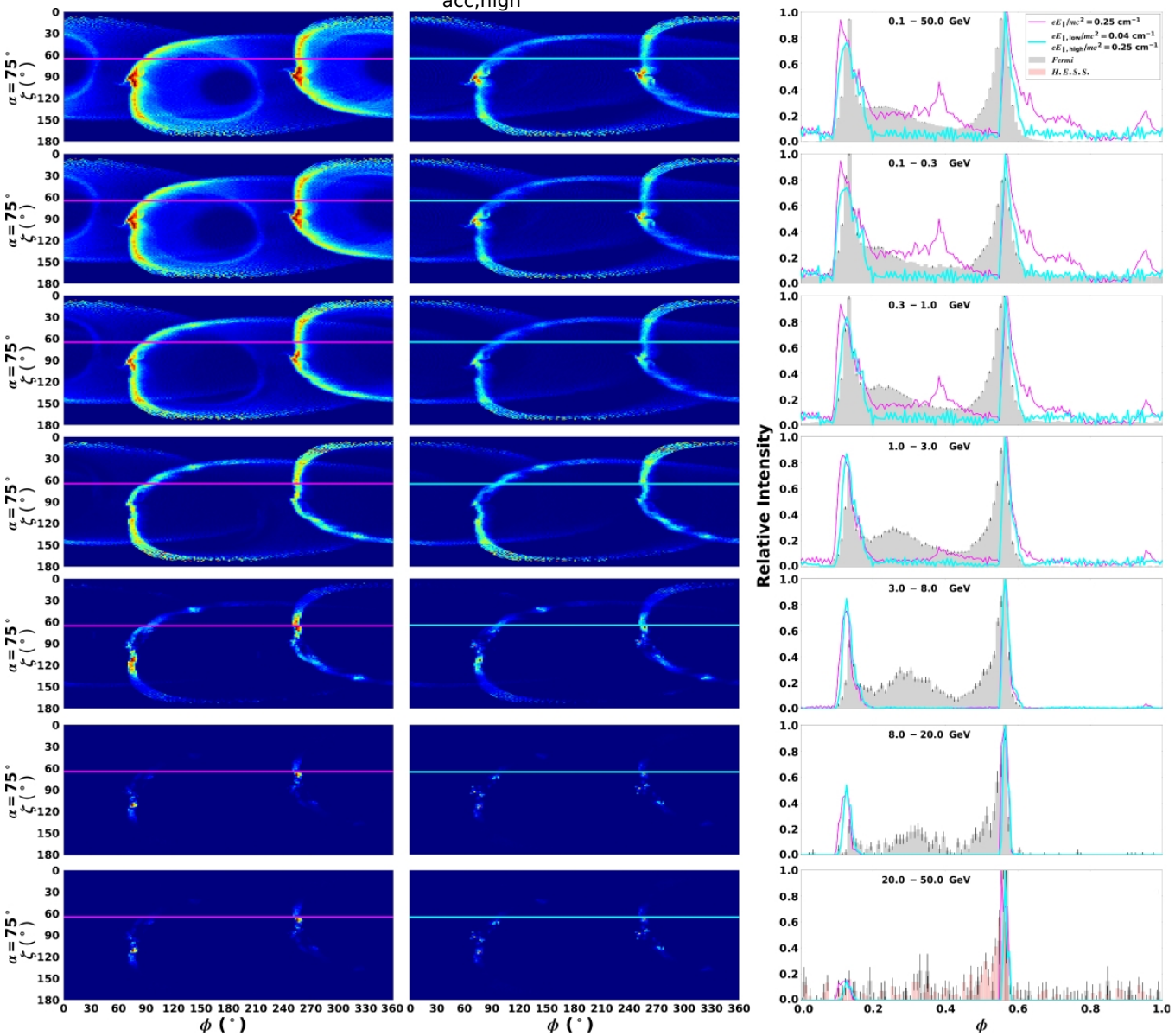

Abdo et al. (2010,2013)
Abdalla et al. (2018)

Energy-dependent curvature light curves

R_{acc} = 0.25 cm^{-1}

$R_{acc,low}$ = 0.04 cm^{-1}
$R_{acc,high}$ = 0.25 cm^{-1}

α = 75°
ζ_{cut} = 40°

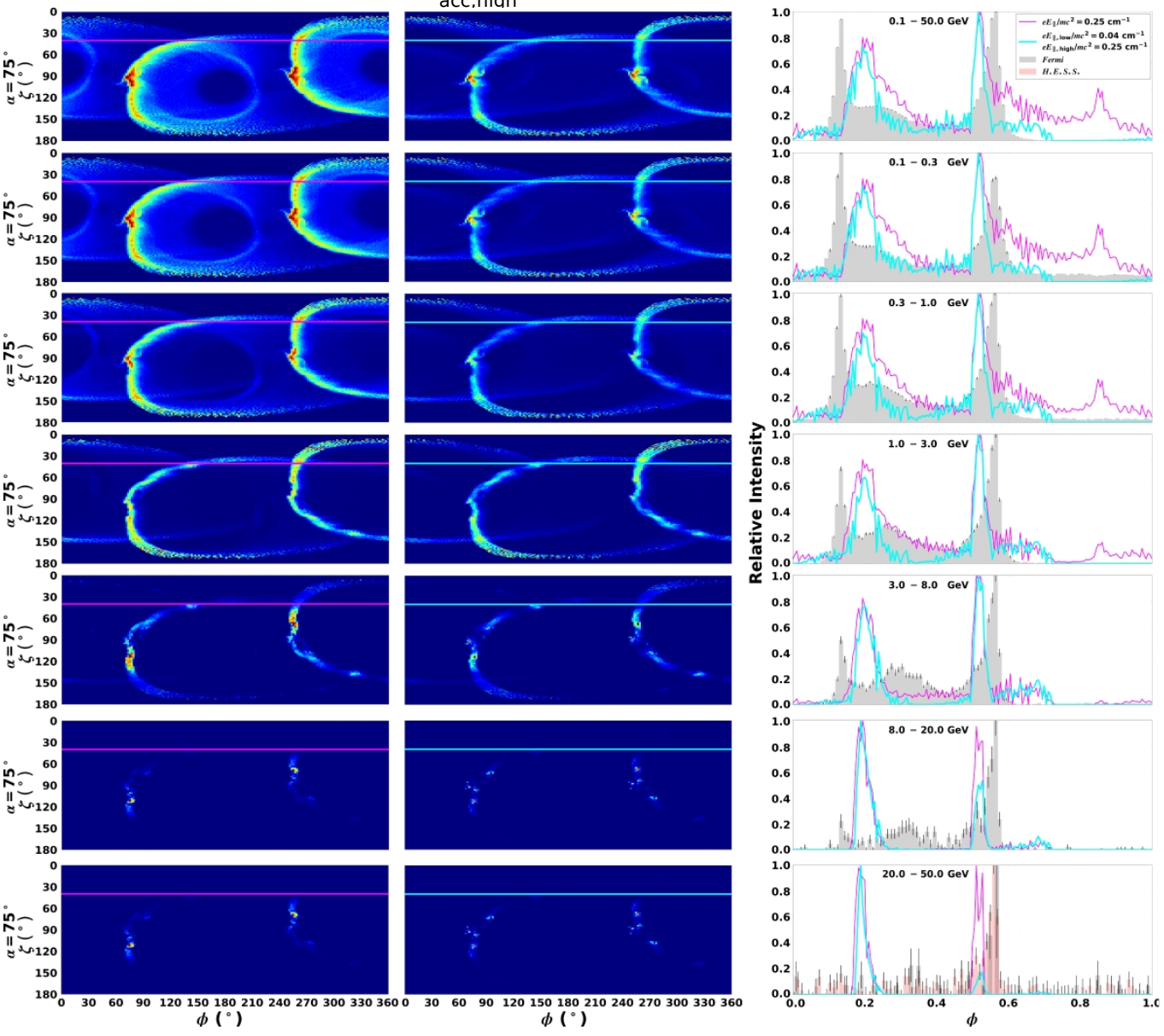

- Test robustness of the P1/P2 vs. photon energy - obtained a counter-example.
- Light curves have a different emission structure due to a different spatial origin of the emission.
- No bridge emission (at high photon energies, see Brambilla et al. 2015).

Abdo et al. (2010,2013)
Abdalla et al. (2018)

Reverse mapping

Barnard et al. (*submitted to ApJ*)

$\alpha = 75^{o}$
$\zeta_{cut} = 65^{o}$
$R_{acc} = 0.25\ cm^{-1}$

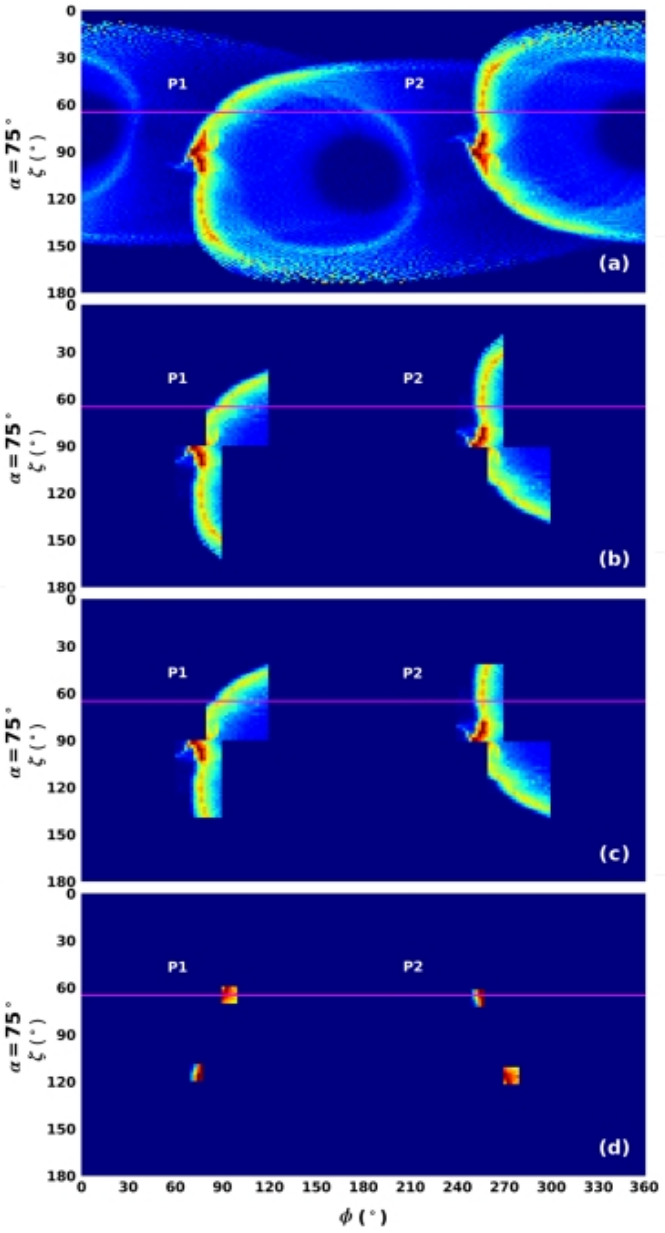

- Isolate P1 and P2:
  - Limit (ϕ,ζ) coordinate values where peaks originate i.e., “blocks”
  - Obtain spatial coordinates (and other parameter quantities) at these coordinates.
- Phase-resolved spectra.
- Need to investigate the local environment where the peaks originate, i.e., energy cutoff ($E_{\gamma,cr}$), curvature radius ($\boldsymbol{\rho}_c$), and Lorentz factor (γ).
- Will explain trends in observed light curves and spectra.

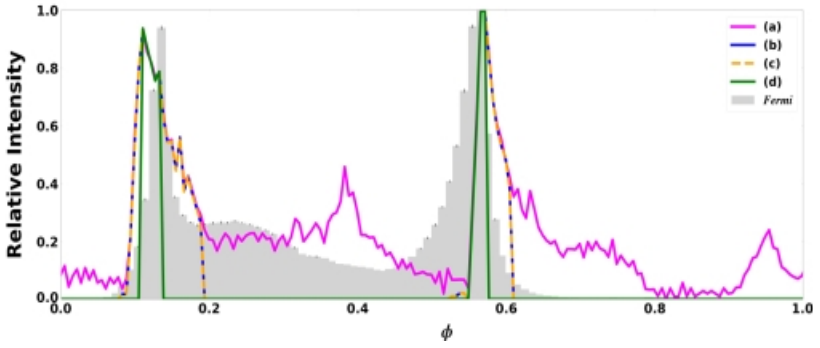

Phase-averaged and resolved CR spectra for Vela

$\alpha = 75^{o}$

$\zeta_{cut} = 65^{o}$

Barnard et al. (*submitted to ApJ*)

$R_{acc} = 0.25\ cm^{-1}$
Norm = $5J_{GJ}$

$R_{acc,low} = 0.04\ cm^{-1}$; $R_{acc,high} = 0.25\ cm^{-1}$
Norm = $8.5J_{GJ}$

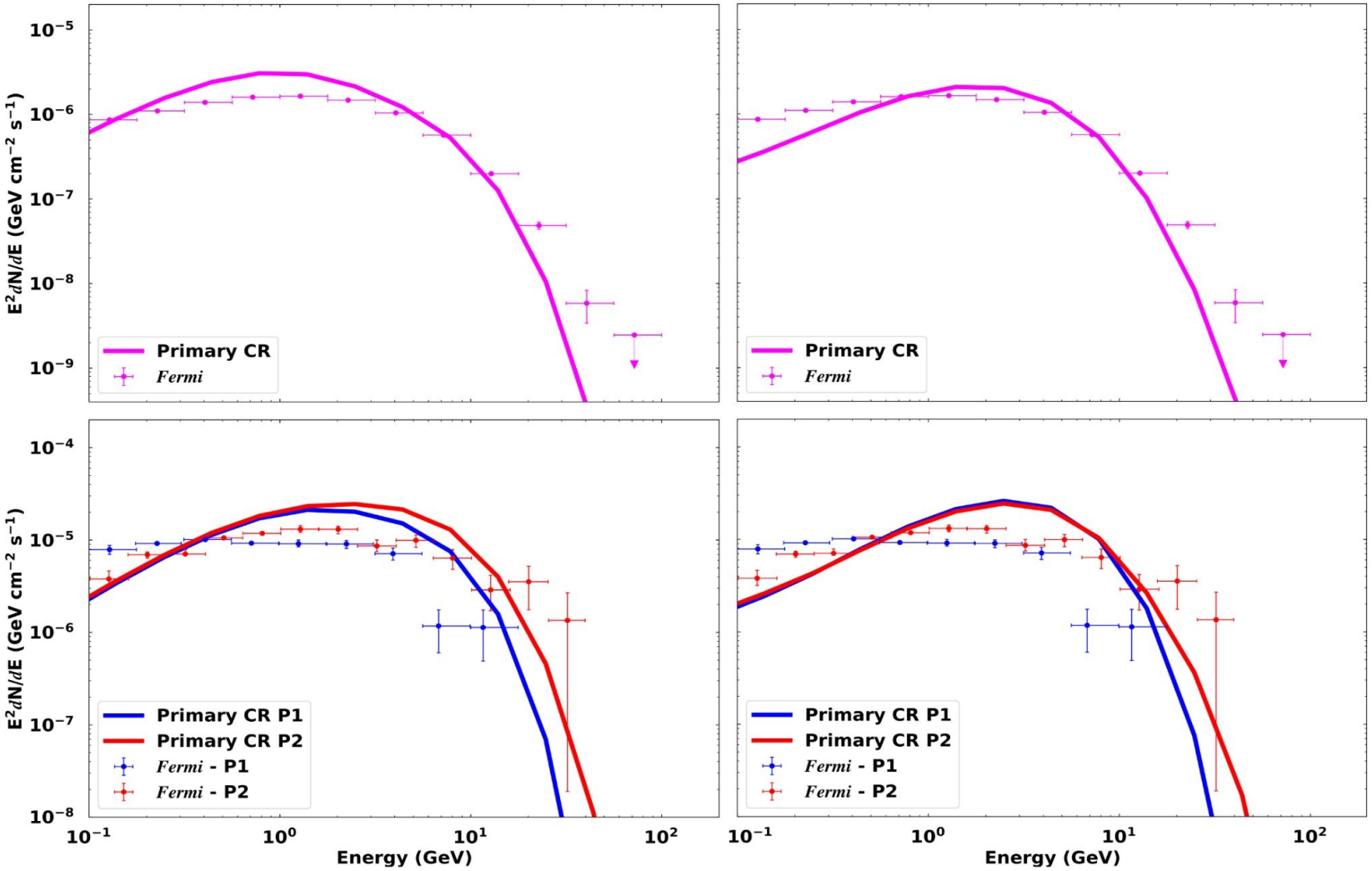

Abdo et al. (2010,2013)

Local environment of emission regions connected to each light curve peak

$$E_{\gamma,\mathrm{CR}} = \frac{3\lambda\!\!\!^{-}_{\mathrm{c}}\gamma^3}{2\rho_{\mathrm{c}}} m_{\mathrm{e}}c^2$$

Barnard et al. (*submitted to ApJ*)

α = 75°
ζ_{cut} = 65°
R_{acc} = 0.25 cm^{-1}

Tails of histograms on the left (same E's)

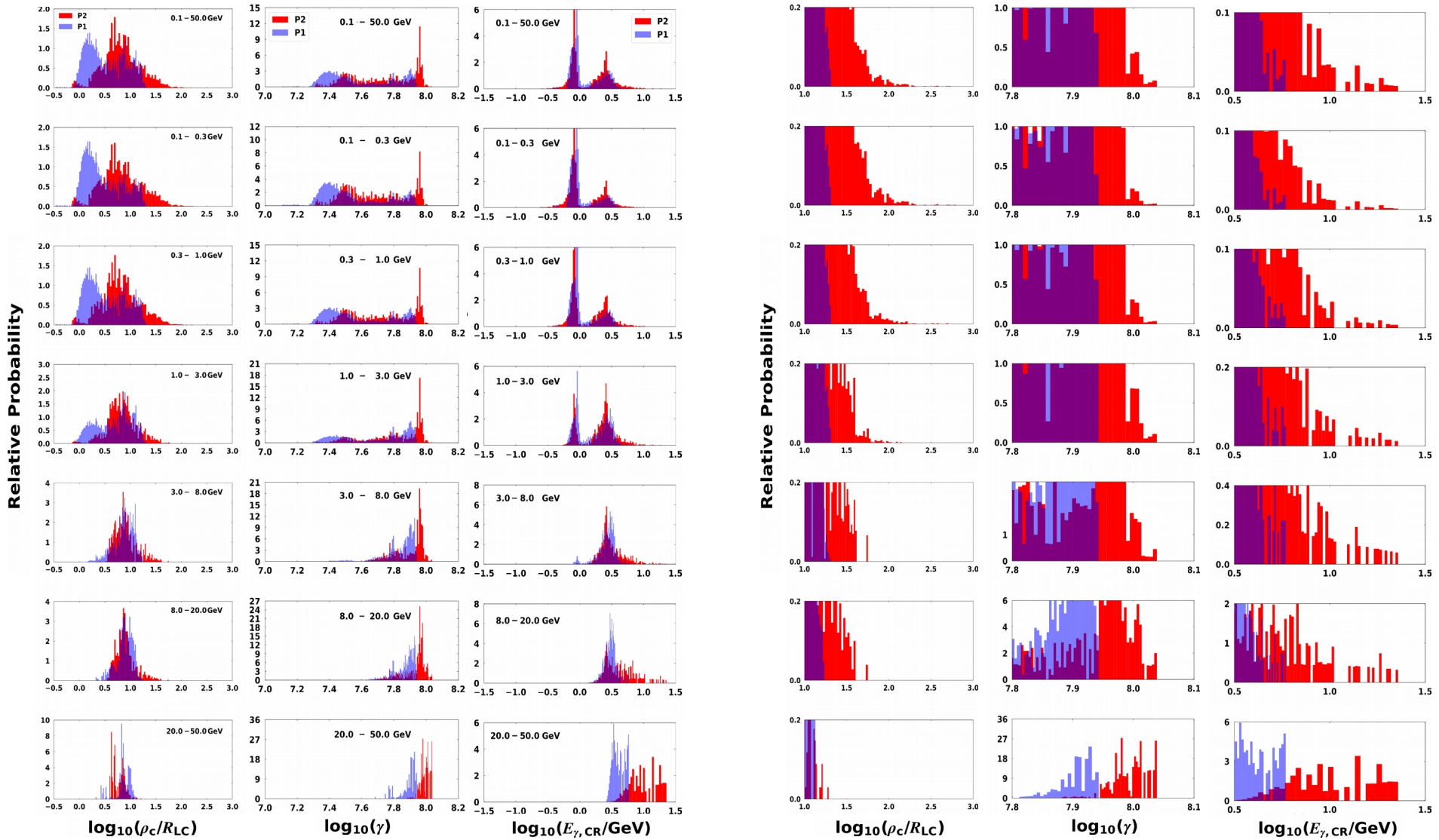

Summary

- For the refined curvature radius - emission caustics are wider, more filled out with radiation, and rounded around the polar caps. The two calculation results are very similar, although the light curves are smoother for the refined calculation.

- Two-step *E*-field: $E_{||,low}$ leads to suppression of emission inside light cylinder as well as disappearance of bridge.

- Our model captures the general trends of the decrease of P1/P2 vs. energy, evolution / suppression of the inter-peak bridge emission, stable peak positions and a decrease in the peak widths as energy is increased.

- We isolate the distribution of Lorentz factors and curvature radii of trajectories associated with the first and second gamma-ray light curve peaks. The median values of these quantities are slightly larger for the second peak, leading to larger cutoffs, and thus explaining the decrease in ratio of first to second peak intensity versus energy.

- Thus, P1/P2 effect is a consequence of the *B*-field structure. Dependence on curvature radius is consistent with CR.

- Ongoing debate regarding the origin of the GeV emission detected from pulsars, it being attributed either to CR or SR (or even IC; see Lyutikov et al. 2012; Lyutikov 2013).

- However, we found reasonable fits to the energy-dependent light curves and phase-resolved spectra of Vela, assuming CR as the mechanism responsible for the GeV emission.

THANKS

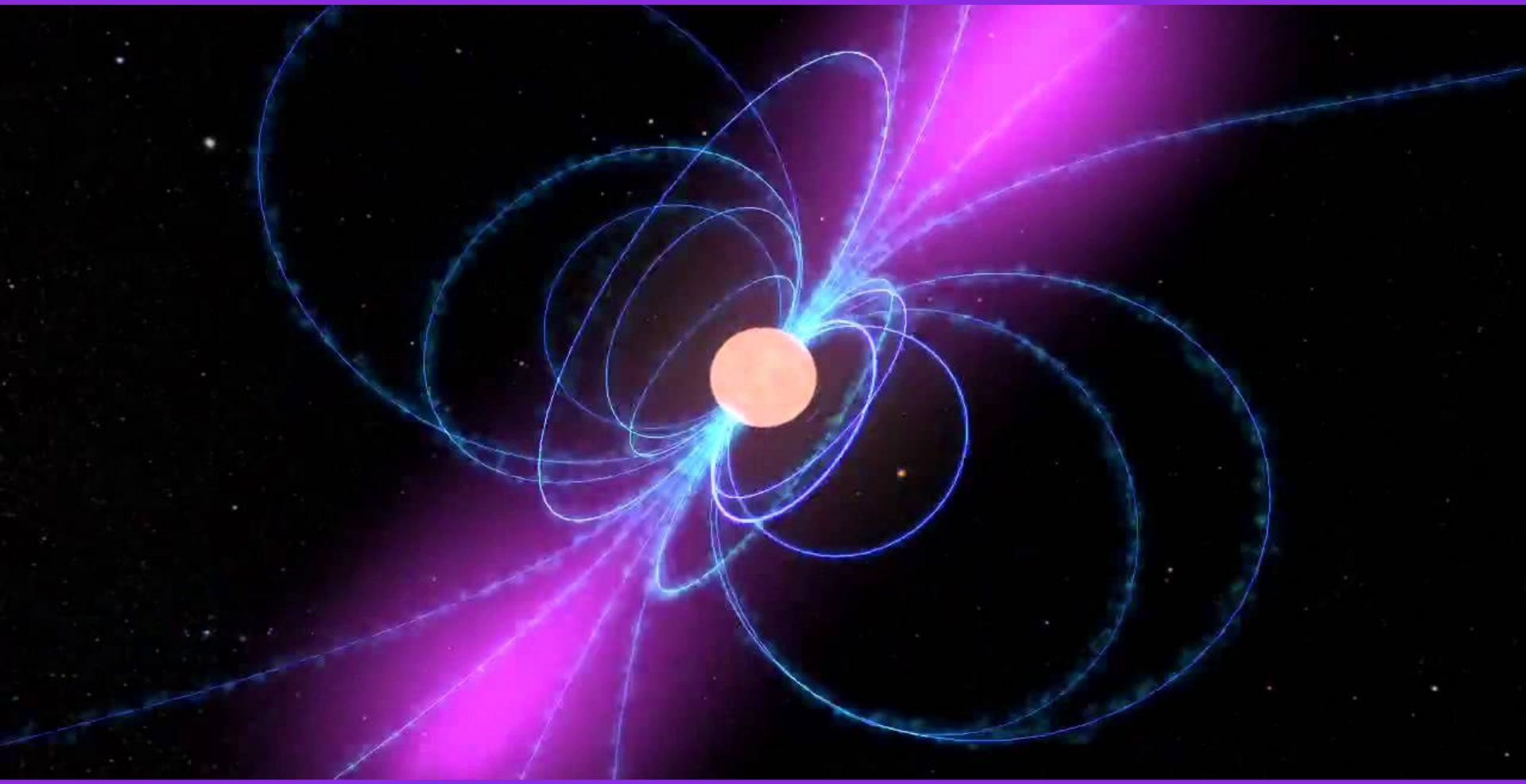

He determines the number of the stars;
He gives to all of them their names.
Psalm 147:4